Size-dependent exchange bias in $La_{0.25}Ca_{0.75}MnO_3$ nanoparticles

X. H. Huang, J. F. Ding, G. Q. Zhang, Y. Hou, Y. P. Yao, and X. G. Li*

Department of Physics, Hefei National Laboratory for Physical Sciences at Microscale, University of Science and Technology of China, Hefei 230026, People's Republic of China and International Center for Materials Physics, Academia Sinica, Shenyang 110015, People's Republic of China

(Received 29 July 2008; revised manuscript received 31 October 2008; published 8 December 2008)

Exchange bias phenomena are observed in $La_{0.25}Ca_{0.75}MnO_3$ nanoparticles with average sizes ranging from 40 to 1000 nm. It is found that the magnetic hysteresis loops display horizontal and vertical shifts in field-cooled processes. The variations of the exchange bias field (H_{EB}) and the coercivity (H_c) with particle size follow nonmonotonic dependencies and show maxima for particles with diameter around 80 nm at $T=5$ K, which can be mainly ascribed to the changes in uncompensated surface spins with nanoparticle size. The peak position for H_c shifts to larger particle size at higher temperature while that for H_{EB} is unconspicuous. The linear relationship between H_{EB} and vertical magnetization shift (M_{EB}) further indicates that the characteristics of uncompensated spins play an important role in the variations of H_{EB} for the manganite.

DOI: 10.1103/PhysRevB.78.224408 PACS number(s): 75.47.Lx, 75.50.Tt, 75.70.Rf

INTRODUCTION

The exchange bias (EB) associated with the exchange coupling at the interface between ferromagnetic (FM) and antiferromagnetic (AFM) spin structures[1–3] has attracted lots of attention due to its potentially technological applications in magnetic devices.[4] The EB effect has been observed in different systems, such as materials containing ferrimagnets (FIs) [e.g., AFM/FI (Ref. 5) and FI/FM (Ref. 6)] or spin-glass (SG) phase [e.g., FM/SG (Ref. 7)], FM/AFM bilayer films,[8] as well as nanoparticles[9–11] due to the exchange coupling between the AFM core and FM shell.

Being typical strongly correlated electron systems, the perovskite-type manganites display many fascinating properties, e.g., colossal magnetoresistance (CMR), charge ordering, and insulator-metal transition, etc.,[12] which have drawn much attention in the last decade. In addition, it is worthwhile to mention that the EB effect has been found recently in manganites such as $Pr_{1/3}Ca_{2/3}MnO_3$,[13] $Y_{0.2}Ca_{0.8}MnO_3$,[14] as well as nanosized $La_{0.7}Ca_{0.3}MnO_3$ (Ref. 15) and $CaMnO_{3-\delta}$ (Ref. 16) and so on, which opens a different field of science and technology for CMR materials. One of the most important issues in this field is how to control the EB effect. It has been reported that the EB effect can be manipulated by cooling magnetic fields[14] or by changing thickness of FM/AFM layers.[17] As for the $Pr_{1/3}Ca_{2/3}MnO_3$ compound,[13] though there exists a large hysteresis loop shift, the inconvenience to control the amount of the FM nanodomains immersed in the AFM background may limit its applications. Therefore, it is still an open question to search for appropriate approaches to manipulate the EB field, which would provide more opportunities in applications for the manganites.

Actually, many researches have revealed that the robust charge ordering in bulk manganites can be weakened in nanoparticles with an appearance of weak ferromagnetism.[18] However, it is not clear whether there exists the EB effect and how to control it in charge-ordered manganites. Our recent research on the charge-ordered $La_{0.25}Ca_{0.75}MnO_3$ nanoparticles[19] demonstrates that the coexistence of FM cluster glass and AFM phases occurs when the particle size is reduced to nanoscale. Thus, the EB effect can be expected in those manganite nanoparticles. For charge-ordered manganites, since the FM interaction alters as the nanoparticle size varies,[19] changing the particle size would be a practical way to tune the EB effect.

In this paper, we studied the temperature and particle diameter (D) dependencies of the exchange bias field (H_{EB}) and coercivity (H_c) of $La_{0.25}Ca_{0.75}MnO_3$ nanoparticles. Our results indicate that H_{EB} and H_c are strongly related to the particle size, which can be well explained on the basis of the uncompensated surface spin related core-shell model.

EXPERIMENT

Polycrystalline nanoparticles of $La_{0.25}Ca_{0.75}MnO_3$ were prepared by a sol-gel method described elsewhere.[19] The crystal structure of each sample was confirmed as an orthorhombic phase by x-ray diffraction (XRD). The field emission scanning electron microscope morphologies of $La_{0.25}Ca_{0.75}MnO_3$ nanoparticles reveal that the sizes of the crystallized particles obtained by different thermal treatments are homogeneous, and the average diameter (D) ranges from 40 to 1000 nm as the annealing temperature increases from 600 to 1280 °C. The magnetization measurements were performed using a superconducting quantum interference device (SQUID) magnetometer. The magnetic hysteresis loops were measured between −50 and 50 kOe after cooling the sample from 300 K to the measuring temperature in zero-field-cooled (ZFC) or field-cooled (FC) processes, and the field for the FC process is 50 kOe. The temperature dependencies of ZFC and FC magnetizations were measured on warming with a magnetic field of 100 Oe, and the field for the FC process is 100 Oe. In the measurement of ZFC magnetization relaxation, the sample was cooled from the room temperature to 50 K without magnetic field, and a field of 100 Oe was applied after different waiting times $t_w=0$, 1000, and 2000 s, then the time evolution of magnetization was recorded.

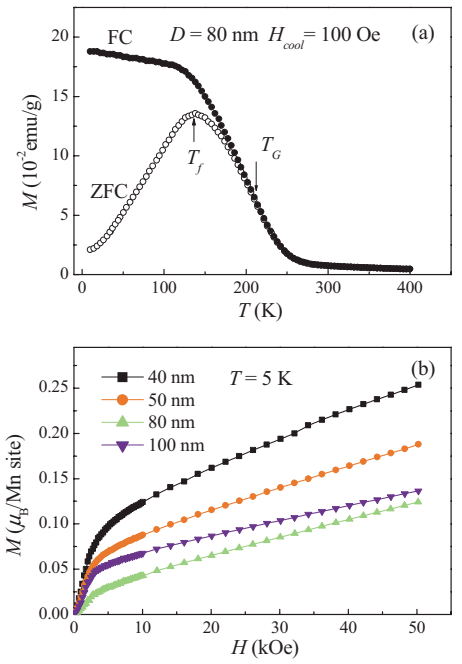

FIG. 1. (Color online) (a) Temperature dependencies of the ZFC and FC magnetizations for the sample with diameter of 80 nm. Both the cooling and measuring fields are 100 Oe. (b) Magnetic field dependencies of magnetizations measured at 5 K for the samples with diameters of 40, 50, 80, and 100 nm.

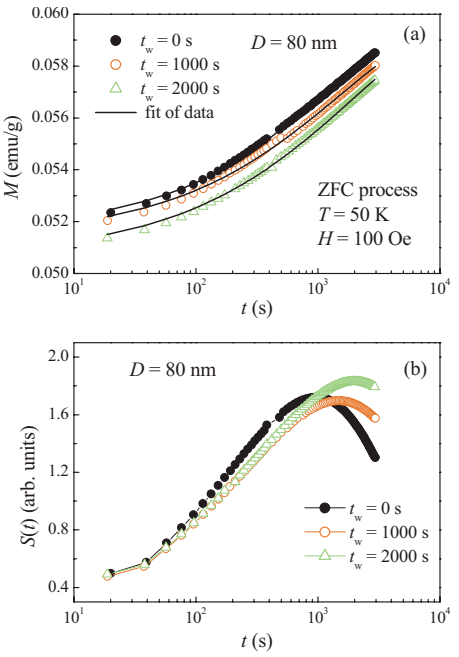

FIG. 2. (Color online) (a) ZFC relaxation magnetizations and (b) the corresponding relaxation rate $S(t)$, for the sample with diameter of 80 nm, measured at 50 K with the waiting time t_w=0, 1000, and 2000 s before using probing field H=100 Oe. Solid lines are the fitting results using Eq. (1).

RESULTS AND DISCUSSION

Figure 1(a) shows the temperature dependencies of magnetizations $M(T)$ for a typical sample with diameter of 80 nm (more details are shown in Ref. 19). With decreasing temperature both ZFC (M_{ZFC}) and FC (M_{FC}) magnetizations rise sharply around the temperature T_G ($T_G \approx 210$ K) that is defined as the minimum of dM/dT vs T curve, suggesting the appearance of a short-range FM coupling and the formation of FM clusters.[20–24] $M_{\mathrm{ZFC}}(T)$ increases gradually to its maximum around a temperature T_f ($T_f \approx 136$ K), and then decreases, while $M_{\mathrm{FC}}(T)$ continues to increase slowly rather than a complete saturation with lowering temperature. All these results indicate that there exists a collective freezing process of the moments of FM clusters, and thus T_f can be regarded as the freezing temperature for the FM clusters. A bifurcation between the FC and ZFC curves usually implies the existence of a cluster glass[24,25] and is possibly due to the magnetic frustration induced by the surface-driven spin frustration and disorder in these nanoparticles,[26–28] which is different from the geometrical frustration occurring in systems with special symmetries and no disorder among the spins.[29] Those phenomena described above exhibit the features of cluster glass systems. On the other hand, the magnetization curves $M(H)$ in Fig. 1(b) measured at 5 K in the ZFC process for the samples with diameter range from 40 to 100 nm show no S shape in the virgin branches, which is out of accord with the behaviors of both canonical SG and reentrant SG systems.[20,21,25] Moreover, in our earlier work, the shift of the peak temperature in ac susceptibility $\chi'(T)$ with measuring frequency[19] implies the existence of a cluster-glass-like state in those nanoparticles.[20,30]

It is worth noting that in the $M(H)$ curve shown in Fig. 1(b) the magnetization value, $0.25\mu_B$/Mn site, measured under 50 kOe for the sample with particle size of 40 nm is much smaller than the $3.25\mu_B$/Mn site (provided that all the Mn ions have FM ordering). Moreover, the magnetization varies almost linearly with $H > 10$ kOe and it does not reach its saturation value even at 50 kOe. All these characteristics indicate the dominant role of the AFM components. Thus, the $La_{0.25}Ca_{0.75}MnO_3$ nanoparticle can be supposed to be composed of an AFM core and FM cluster-glass-like shell. As the temperature is lowered through T_G, the finite-range ferromagnetic ordering is constructed in the shell, and the FM clusters form and begin to freeze around T_f. Though the Néel temperature (T_N) could not be confirmed from the ZFC M-T curve due to the superposition of the FM and AFM moments under the applied field of 100 Oe,[19] the exchange coupling between FM and AFM interfaces would be expected at a low temperature in those particles.

In order to further confirm the magnetic state of the sample, the magnetization relaxation was performed at a temperature well below the freezing temperature T_f. It can be clearly seen from Fig. 2(a) that the time-dependent relaxation $M(t)$ of the ZFC magnetization depends on the waiting time t_w and can be described by the stretched exponential function,[24,25]

$$M(t) = M_0 - M_r \exp\left[-\left(\frac{t}{\tau_r}\right)^{1-n}\right], \tag{1}$$

where M_0 and M_r are related to an intrinsic FM component and glassy component, respectively, τ_r represents a time con-

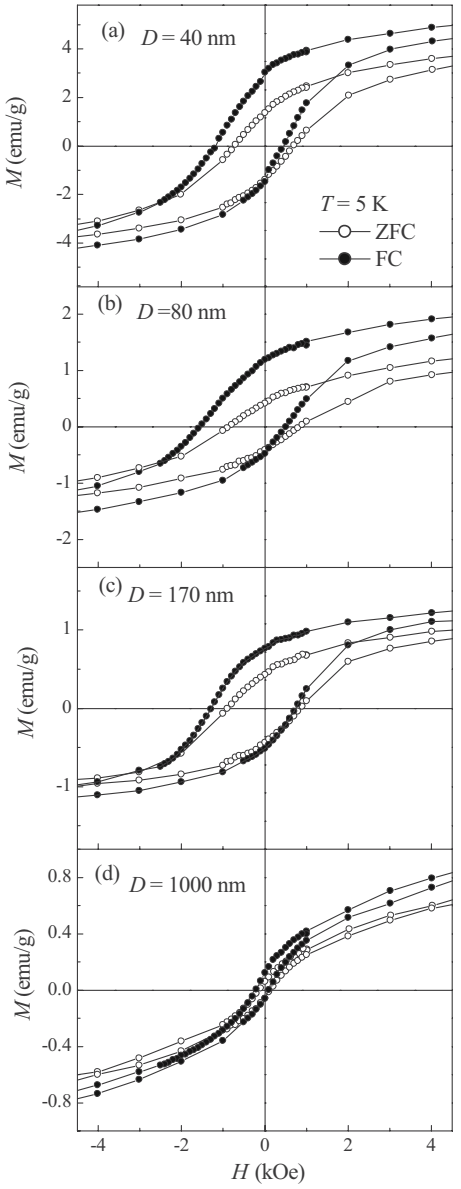

FIG. 3. Typical M-H curves of the samples with diameters of 40, 80, 170, and 1000 nm measured at 5 K in the ZFC and FC cases with H_{cool}=50 kOe.

stant, and n is a parameter. The corresponding relaxation rate, defined as $S(t)=\partial M/\partial(\ln t)$,[25] was obtained by taking the derivative of the polynomial fit of the magnetization data, which is plotted in Fig. 2(b). A peak appears in the $S(t)$ curve and shifts to longer observation time for longer waiting time, which indicates the age-dependent effect and is often observed in other cluster glass systems.[25,31]

Figure 3 shows the magnetic hysteresis loops of the samples with different particle sizes measured at 5 K under both ZFC and FC modes. One can see that in the FC process the hysteresis loops shift toward the negative field and the positive magnetization, while in the ZFC case the loops are still centered about the origin. As aforementioned that a physical picture for $La_{0.25}Ca_{0.75}MnO_3$ nanoparticles is demonstrated by a core-shell model, the presence of the microscopic unidirectional exchange anisotropy interaction at the

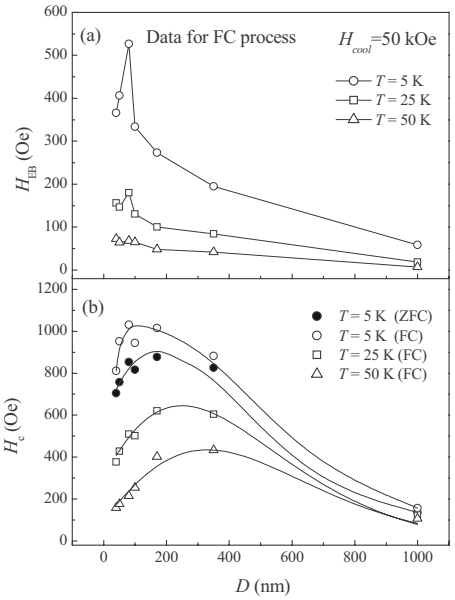

FIG. 4. (a) Average particle diameter dependencies of exchange bias field H_{EB} measured at 5, 25, and 50 K in FC processes. (b) Average particle diameter dependencies of the coercivity measured at 5 K in ZFC and FC processes, and at 25 and 50 K in FC process. The solid lines are guides for the eyes.

FM/AFM interface is responsible for the exchange bias phenomena.[1] As the sample is cooled down through T_G in the FC process, the FM cluster spins of the shell align along the direction of magnetic field H_{cool} and freeze at low temperatures. The interfacial FM clusters on the exterior surface of the AFM core tend to be coupled with AFM spins at the interface as the temperature is lowered through T_N,[1–3] and thus the exchange bias appears. Usually, the shift related to the exchange bias field is defined as $H_{EB}=|H_1+H_2|/2$ and the coercivity as $H_c=|H_1-H_2|/2$, where H_1 and H_2 denote the left and right coercivity fields, respectively.[13] Figures 4(a) and 4(b) show the diameter (D) dependencies of H_{EB} and H_c at different temperatures. It can be seen that H_{EB} and H_c at 5 K increase with decreasing D, reach their maxima around 80 nm, and then decrease. With increasing temperature, H_{EB} decreases and the peak height diminishes gradually but the peak position changes unconspicuously. However, it is clear that with increasing temperature the peak position of H_c shifts to larger particle size.

It is believed that the exchange coupling is closely related to the interfacial uncompensated spins. For $La_{0.25}Ca_{0.75}MnO_3$ nanoparticles, as the particle size decreases, more and more surface spins deviate from the AFM arrangement,[19,32] which implies the increasing proportion of the uncompensated spin shell and the reduction in the AFM core in the nanoparticle. Meanwhile, the uncompensated surface spins favor the FM coupling, leading to the increase in FM clusters with reducing particle size. However, with further decreasing particle size, the AFM anisotropy energy reduces, and so the FM/AFM interfacial pinning strength on the FM spins is weakened; meanwhile more disordered surface spins weaken the FM coupling.[19] Thus, H_{EB} increases first, and reaches its maximum, then decreases with decreasing particle size.

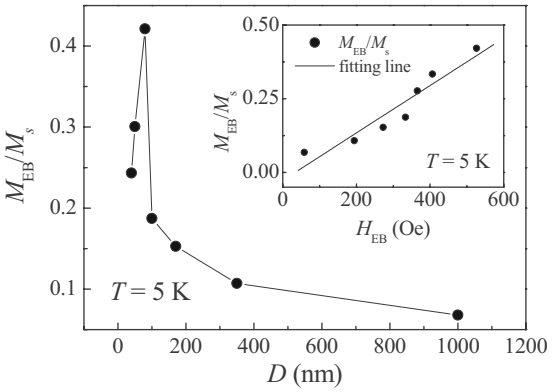

FIG. 5. Average particle diameter dependence of M_{EB}/M_s measured at 5 K in FC process. Inset: Relationship between H_{EB} and M_{EB}/M_s at 5 K. The solid line is the linear fit.

As we know, Malozemoff[33] proposed a random-field model to describe AFM layer thickness dependence of H_{EB} for FM-AFM films in which H_{EB} shows a peak at a certain AFM layer thickness. Thus, the presence of AFM domains can account for the particle size dependence of H_{EB} by an argument analogous to the one for AFM layer thickness dependence of FM-AFM films.[5,34–36] However, the variation tendency of H_{EB} with particle size at different temperatures [shown in Fig. 4(a)] in the $La_{0.25}Ca_{0.75}MnO_3$ nanoparticles is different from the findings in the FM-AFM films, such as the Co/IrMn system where the peak in H_{EB} shifts to larger thickness of the AFM layer with increasing temperature.[36] The reasons are probably due to the following two aspects. (1) For $La_{0.25}Ca_{0.75}MnO_3$ nanoparticles the fraction of FM clusters in the shell is different at different particle size,[19] whereas the FM layer thickness in the FM-AFM films is fixed.[36,37] (2) Both the FM coupling and the interaction between FM clusters in the shell and AFM core will be different for nanoparticles with different sizes. Thus, in the $La_{0.25}Ca_{0.75}MnO_3$ nanoparticles, both the fraction of FM components in the shell and the AFM anisotropy in the core alter with increasing temperature, giving rise to the unconspicuous change in the peak position in H_{EB}.

From the discussions mentioned above, it is also reasonable to find a peak for the particle size dependence of $H_c(D)$ in the ZFC case [see Fig. 4(b)] because the coercivity is closely related to the FM ordering.[38] In fact, for a sufficiently small particle size, though the anisotropy of the AFM core becomes smaller, more disordered uncompensated spins appear, and thus the FM coupling is weakened,[19,39] which will result in the decrease in H_c and thus a peak occurs in the H_c vs D curve. The enhanced H_c observed in the FC process is usually attributed to the largely enhanced unidirectional anisotropy of FM clusters in the FM/AFM interface;[2,3] the FM spins can drag more interfacial AFM spins, leading to the increase in H_c. The reason why the peak position of H_c of the system shifts to a larger particle size with increasing temperature is still not very clear and more investigations are needed in the future.

The particle size dependence of M_{EB}/M_s obtained at 5 K shown in Fig. 5 exhibits a similar trend as that of H_{EB}. Here, the remanence asymmetry M_{EB} corresponding to the vertical

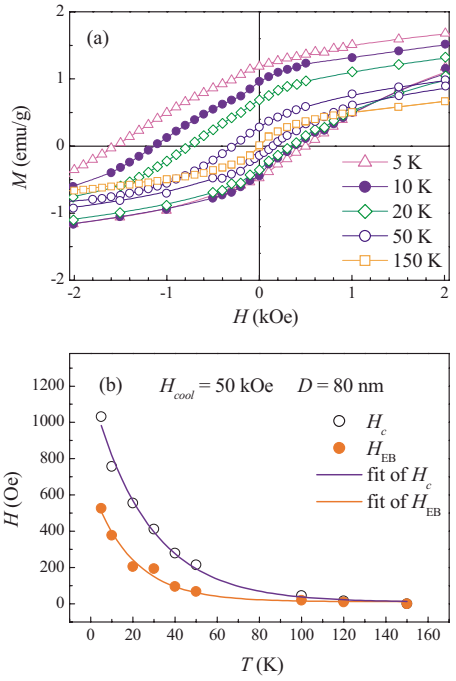

FIG. 6. (Color online) (a) M-H curves measured at different temperatures in the FC case. (b) Temperature dependencies of H_{EB} and H_c in the FC process. The solid lines are the fits using Eq. (2).

magnetization shift is defined as $M_{EB}=|M_1+M_2|/2$, where M_1 and M_2 represent the positive and negative remanent magnetizations, respectively, and M_s is the saturation magnetization after the AFM moment is subtracted. One can find that there is a nearly linear relationship between H_{EB} and M_{EB}/M_s, as shown in the inset of Fig. 5. The fitting line indicates that a linear relationship deduced for polycrystalline samples[13] is still suitable in the case of $La_{0.25}Ca_{0.75}MnO_3$ nanoparticles. It is reported that the vertical shift M_{EB} is ascribed to the pinned spins at the interface,[40–42] of which the number is a measure of the vertical shift. Therefore, the linear relation described above indicates the dependence of H_{EB} on the interfacial uncompensated spins in $La_{0.25}Ca_{0.75}MnO_3$ nanoparticles.

The temperature dependencies of H_{EB} and H_c obtained from magnetic hysteresis loops (M vs H) in the temperature range from 5 to 150 K for the sample with diameter of 80 nm were studied in the FC process, as shown in Fig. 6. One can see from Fig. 6(a) that the hysteresis loop becomes narrower with increasing temperature. As presented in Fig. 6(b), the temperature dependencies of H_{EB} and H_c can be fitted using the formula as[43]

$$H_{EB} = H_{EB}(0)\exp(-T/T_1),$$

$$H_c = H_c(0)\exp(-T/T_2), \tag{2}$$

where $H_{EB}(0)$ and $H_c(0)$ are the extrapolations of H_{EB} and H_c to the absolute zero temperature; T_1 and T_2 are constants. With increasing temperature, the AFM order is diminished due to the thermal fluctuations, which results in the weakening interfacial interaction and then reducing the loop shift along the field direction. When the temperature approaches

T_N of the $La_{0.25}Ca_{0.75}MnO_3$ compound, H_{EB} vanishes due to the disappearance of AFM order.

CONCLUSION

In summary, the EB effect is observed in $La_{0.25}Ca_{0.75}MnO_3$ nanoparticles with different diameters. Both H_{EB} and H_c are nonmonotonously dependent on D and exhibit their maxima around $D=80$ nm at $T=5$ K. The changes in uncompensated spins and AFM domains for different particle sizes are responsible for the behaviors of H_{EB} and H_c. As the temperature increases, the peaks in $H_{EB}(D)$ and $H_c(D)$ exhibit different trends; this needs more investigations to figure out the mechanism. Our results provide a method to tune H_{EB} by changing the particle sizes and then expand the application scope and fundamental understanding of the EB effect for CMR manganites.

ACKNOWLEDGMENTS

This work was supported by the National Natural Science Foundation of China (Grants No. 50721061 and No. 50832007) and the National Basic Research Program of China (Grant No. 2006CB922005 and No. 2009CB929502).

*lixg@ustc.edu.cn

[1] J. Nogués, J. Sort, V. Langlais, V. Skumryev, S. Suriñach, J. S. Muñoz, and M. D. Baró, Phys. Rep. **422**, 65 (2005).
[2] A. E. Berkowitz and Kentaro Takano, J. Magn. Magn. Mater. **200**, 552 (1999).
[3] J. Nogués and Ivan K. Schuller, J. Magn. Magn. Mater. **192**, 203 (1999).
[4] S. Parkin, X. Jiang, C. Kaiser, A. Panchula, K. Roche, and M. Samant, Proc. IEEE **91**, 661 (2003).
[5] G. Salazar-Alvarez, J. Sort, S. Suriñach, M. Dolors Baró, and J. Nogués, J. Am. Chem. Soc. **129**, 9102 (2007).
[6] W. C. Cain and M. H. Kryder, J. Appl. Phys. **67**, 5722 (1990).
[7] M. Ali, P. Adie, C. H. Marrows, D. Greig, B. J. Hickey, and R. L. Stamps, Nature Mater. **6**, 70 (2007).
[8] P. Miltényi, M. Gierlings, M. Bamming, U. May, G. Güntherodt, J. Nogués, M. Gruyters, C. Leighton, and Ivan K. Schuller, Appl. Phys. Lett. **75**, 2304 (1999).
[9] M. S. Seehra and A. Punnoose, Solid State Commun. **128**, 299 (2003).
[10] R. H. Kodama, S. A. Makhlouf, and A. E. Berkowitz, Phys. Rev. Lett. **79**, 1393 (1997).
[11] C. H. Ho and C. H. Lai, IEEE Trans. Magn. **42**, 3069 (2006).
[12] E. Dagotto, *Nanoscale Phase Separation and Colossal Magnetoresistance* (Springer, Berlin, 2003).
[13] D. Niebieskikwiat and M. B. Salamon, Phys. Rev. B **72**, 174422 (2005).
[14] T. Qian, G. Li, T. Zhang, T. F. Zhou, X. Q. Xiang, X. W. Kang, and X. G. Li, Appl. Phys. Lett. **90**, 012503 (2007).
[15] M. Muroi, P. G. McCormick, and R. Street, Rev. Adv. Mater. Sci. **5**, 76 (2003).
[16] V. Markovich, I. Fita, A. Wisniewski, R. Puzniak, D. Mogilyansky, L. Titelman, L. Vradman, M. Herskowitz, and G. Gorodetsky, Phys. Rev. B **77**, 054410 (2008).
[17] I. Panagiotopoulos, C. Christides, M. Pissas, and D. Niarchos, Phys. Rev. B **60**, 485 (1999).
[18] S. Dong, F. Gao, Z. Q. Wang, J. M. Liu, and Z. F. Ren, Appl. Phys. Lett. **90**, 082508 (2007).
[19] T. Zhang, T. F. Zhou, T. Qian, and X. G. Li, Phys. Rev. B **76**, 174415 (2007).
[20] S. Mukherjee, R. Ranganathan, P. S. Anilkumar, and P. A. Joy, Phys. Rev. B **54**, 9267 (1996).
[21] M. Itoh, I. Natori, S. Kubota, and K. Motoya, J. Phys. Soc. Jpn. **63**, 1486 (1994).
[22] X. G. Li, X. J. Fan, G. Ji, W. B. Wu, K. H. Wong, C. L. Choy, and H. C. Ku, J. Appl. Phys. **85**, 1663 (1999).
[23] D. Parker, V. Dupuis, F. Ladieu, J.-P. Bouchaud, E. Dubois, R. Perzynski, and E. Vincent, Phys. Rev. B **77**, 104428 (2008).
[24] Y.-K. Tang, Y. Sun, and Z.-H, Cheng, J. Phys.: Condens. Matter **20**, 095208 (2008).
[25] R. S. Freitas, L. Ghivelder, F. Damay, F. Dias, and L. F. Cohen, Phys. Rev. B **64**, 144404 (2001).
[26] J. M. D. Coey, Phys. Rev. Lett. **27**, 1140 (1971).
[27] R. H. Kodama, A. E. Berkowitz, E. J. McNiff, and S. Foner, Phys. Rev. Lett. **77**, 394 (1996).
[28] *Surface Effects in Magnetic Nanoparticles*, edited by D. Fiorani (Kluwer, Dordrecht, 2005).
[29] A. P. Ramirez, Annu. Rev. Mater. Sci. **24**, 453 (1994).
[30] J. A. Mydosh, *Spin Glass: An Experimental Introduction* (Taylor and Francis, London, 1993).
[31] D. N. H. Nam, K. Jonason, P. Nordblad, N. V. Khiem, and N. X. Phuc, Phys. Rev. B **59**, 4189 (1999).
[32] R. N. Bhowmik, R. Nagarajan, and R. Ranganathan, Phys. Rev. B **69**, 054430 (2004).
[33] A. P. Malozemoff, Phys. Rev. B **35**, 3679 (1987); **37**, 7673 (1988).
[34] V. Baltz, J. Sort, S. Landis, B. Rodmacq, and B. Dieny, Phys. Rev. Lett. **94**, 117201 (2005).
[35] V. Baltz, J. Sort, B. Rodmacq, B. Dieny, and S. Landis, Phys. Rev. B **72**, 104419 (2005).
[36] M. Ali, C. H. Marrows, M. Al-Jawad, B. J. Hickey, A. Misra, U. Nowak, and K. D. Usadel, Phys. Rev. B **68**, 214420 (2003).
[37] J. van Driel, F. R. de Boer, K.-M. H. Lenssen, and R. Coehoom, J. Appl. Phys. **88**, 975 (2000).
[38] J. W. Cai, Kai Liu, and C. L. Chien, Phys. Rev. B **60**, 72 (1999).
[39] S. S. Rao, S. Tripathi, D. Pandey, and S. V. Bhat, Phys. Rev. B **74**, 144416 (2006).
[40] A. Ceylan, C. C. Baker, S. K. Hasanain, and S. I. Shah, J. Appl. Phys. **100**, 034301 (2006).
[41] J. Nogués, C. Leighton, and Ivan K. Schuller, Phys. Rev. B **61**, 1315 (2000).
[42] R. K. Zheng, G. H. Wen, K. K. Fung, and X. X. Zhang, Phys. Rev. B **69**, 214431 (2004).
[43] N. Moutis, C. Christides, I. Panagiotopoulos, and D. Niarchos, Phys. Rev. B **64**, 094429 (2001).